

MANIPULATION OF LARGE FLEXIBLE STRUCTURAL MODULES BY SPACE ROBOTS MOUNTED ON FLEXIBLE STRUCTURES

Dimitrios Tzeranis¹, Yoshiyuki Ishijima², Steven Dubowsky¹

(1) MIT, 77 Massachusetts Avenue #3-469, Cambridge, MA 02139, USA, {tzeranis,dubowsky}@mit.edu

(2) Japan Aerospace Exploration Agency, 2-1-1, Sengen, Tsukuba, Ibaraki, 305-8505, Japan,
ishijima.yoshiyuki@jaxa.jp

ABSTRACT

Future large space structures (LSS) will be constructed on orbit by assembling large subassemblies using teams of robots. Here, the challenging task of the control and planning of the cooperative manipulation of large flexible structural modules by such teams is addressed. The robots are mounted on the compliant LSS while moving a module to its pre-assembly position. The objective is to position the module accurately and to minimize the induced vibration in the large structure and the module. A method is developed to control the forces applied by the robots to the module and their support structures, which exploits robot cooperation and redundancy. The method is evaluated using simulations.

1. INTRODUCTION

Future space solar power stations (SSPS) are expected to be an important power source [1]. Due to their large size, they will need to be constructed on orbit by space robots since human extra-vehicle activity (EVA) is expensive and dangerous [2].

Studies of the robotic construction of LSS have largely focused on the assembly of truss structures by small simple structural elements and on the design of space structure components [3, 4]. However, the problem of using robots to manipulate and assemble large flexible sub-structures has not been well addressed. Related work can be found in the cooperative manipulation of flexible objects and in the planning and control of robots on compliant bases [5, 6, 7].

Here, the problem of cooperative manipulation of a large flexible object by a team of robots mounted on the LSS under construction is considered. The objective is to design a planning and control algorithm that permits robots to manipulate the structural module precisely while inducing low levels of vibration in the module and the robot compliant base structures, Fig 1.

The proposed approach uses measurements of the forces/torques applied by the robots to the module and

the LSS and exploits robot cooperation and redundancy to plan and control the forces applied by the robots to the module and the LSS.

Simulation results show the effectiveness of the approach in positioning the module precisely while maintaining low levels of residual vibration in the module and the large structure. The analysis also provides guidelines for the robot design that enhance its ability to apply the proposed method.

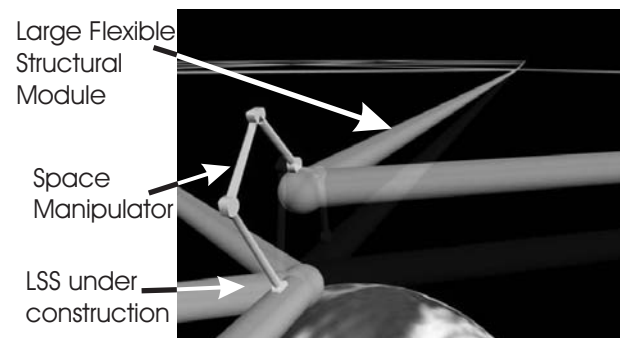


Fig. 1 : Concept picture for the construction of LSS by space robots mounted on flexible structures.

2. PROBLEM DEFINITION

2.1 Task Description

Future LSS will be constructed by assembling large structural modules on orbit [1]. Every module needs to be positioned into its precise pre-assembly position so that it can be assembled into the LSS probably using automatic connection mechanisms [4]. This manipulation task will be carried out by space manipulators mounted on the LSS. This is a challenging cooperative manipulation task due to the size and flexibility of the LSS modules and the flexibility of the LSS that supports the robots.

A simple planar model of such a system is shown in Fig. 2. Two rigid link redundant robots (estimated size 20m) maneuver a long (estimated size 100 to 200 m) flexible structural module from some initial position (about 8m

from the LSS) to its pre-assembly position (less than 1m from the LSS). The robots are mounted on the LSS under construction. The drawing is not to scale as the module is likely to be an order of magnitude larger than the robot. The objective is to use robots to position the module precisely into its desired position, in given time (about 30-60 seconds), while inducing minimal levels of vibration to the module and the robot base structure. While the examples considered in this paper are planar, the approach can be extended to the more general three-dimensional case.

Fig. 3b shows an example LSS concept configuration considered in this study. The structure diameter is approximately two kilometres. For such a planar-like structure, the structure stiffness in the plane of the structure is much larger than the stiffness normal to this plane.

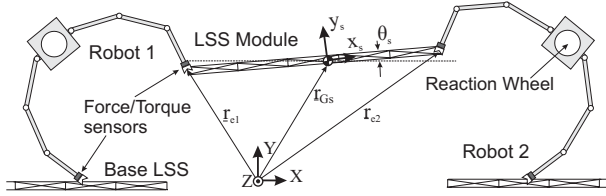


Fig. 2. System model

2.2 System Model

Each robot is assumed to have N rigid links and a reaction wheel whose axis is parallel to the Z axis, Fig 2. It is assumed that each robot has at least three links and that it grasps the beam firmly at its ends. Each robot applies forces to the module but not torques (the connection acts as a pinned joint). The state of each robot is described by its joint angle vector $\underline{\theta}_i$, where $i=1$ refers to the left robot and $i=2$ to the right robot. $\underline{\tau}_i$ denotes the torques applied at the joints of robot i , \underline{f}_{si} is the force applied by robot i to the module and \underline{J}_{ei} is the Jacobian for the position \underline{r}_{ei} of robot i end-effector:

$$\dot{\underline{r}}_{ei} = \underline{J}_{ei} \dot{\underline{\theta}}_i \quad (1)$$

The robot dynamics written in operation space (coincides with the inertial frame XYZ) are [8]:

$$\underline{B}_{Ai} \ddot{\underline{r}}_{ei} + \underline{\eta}_{Ai} + \underline{D}_{Ai} \dot{\underline{r}}_{ei} = \underline{\gamma}_i - \underline{f}_{si} \quad (2)$$

where $\underline{\eta}_{Ai}$ are nonlinear terms and \underline{B}_{Ai} , \underline{D}_{Ai} are the manipulator inertia and damping matrices with respect to its operation space. The vector $\underline{\gamma}_i$ is the contribution of the end-effector forces due to joint actuation $\underline{\tau}_i$:

$$\underline{\tau}_i = \underline{J}_{ei}^T \underline{\gamma}_i \quad (3)$$

The reaction forces \underline{f}_{bi} and moments $\underline{\mu}_{bi}$ exerted to the LSS by the robot are (assuming slow base motion):

$$\begin{bmatrix} \underline{f}_{bi} \\ \underline{\mu}_{bi} \end{bmatrix} = -\frac{d}{dt} \begin{bmatrix} \underline{L}_i \\ \underline{H}_i \end{bmatrix} - \begin{bmatrix} \underline{r}_{Gei} \times \underline{f}_{si} - \underline{r}_{Gbi} \times \underline{f}_{bi} \end{bmatrix} \quad (4)$$

where \underline{L}_i , \underline{H}_i are the robot linear and angular momentum and \underline{r}_{Gei} , \underline{r}_{Gbi} are vectors starting from the robot centre of mass and ending at its end-effector and base respectively.

The module is assumed to be constructed from slender rods and cable and can be modelled as a long Euler-Bernoulli beam, Fig. 3a. The beam “rigid body” motion is described by its orientation θ_s and the inertial position \underline{r}_{Gs} of its centre of mass, Fig 2. Given the nature of the task considered here, θ_s and $\dot{\theta}_s$ are assumed to be relatively small. It is also assumed that the effect of orbital mechanics is negligible, that the kinematic and dynamic parameters of the module are relatively well known and that initially the beam has no vibration. The beam vibration displacement \underline{u}_s is approximated by the rigid body motion and the first N modes of the free-free beam through the assumed modes method [9]. The corresponding equations for the dynamics of the free-free beam are:

$$\underline{M}_s \ddot{\underline{x}}_s = \underline{W}_{sr} \begin{bmatrix} \underline{f}_{s1} \\ \underline{f}_{s2} \end{bmatrix}^T \quad (5)$$

$$\ddot{\underline{q}}_s + 2\underline{Z}\underline{\Omega}\dot{\underline{q}}_s + \underline{\Omega}^2 \underline{q}_s = \underline{W}_{sv} \begin{bmatrix} \underline{f}_{s1} \\ \underline{f}_{s2} \end{bmatrix} = \begin{bmatrix} h_1(t) \\ \dots \\ h_N(t) \end{bmatrix} \quad (6)$$

where $\underline{x}_s = \begin{bmatrix} \underline{r}_{Gs}^T & \theta_s \end{bmatrix}^T$ is the beam rigid body state, \underline{M}_s is the beam mass matrix, \underline{Z} and $\underline{\Omega}$ are the beam modal damping and natural frequency matrices, and \underline{W}_{sr} , \underline{W}_{sv} are grasp matrices [10].

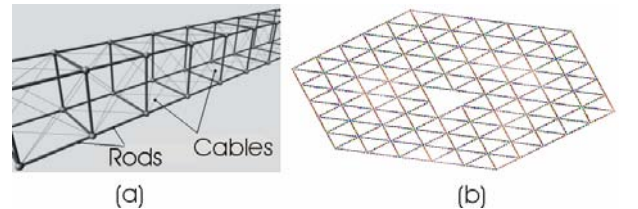


Fig. 3. Sample LSS structural module (a) and LSS under construction (b)

3. APPROACH OVERVIEW

In the proposed approach, called “Vibration Minimization using Redundancy” (VMR), robots plan

and control the forces they apply to the module and the LSS through closed loop force controllers, Fig. 4. The robots plan and control the forces \underline{f}_{si} they apply to the module cooperatively so that the module is positioned accurately and with low levels of residual vibration. Each robot exploits its redundancy to plan and control the reaction forces \underline{f}_{bi} and torques $\underline{\mu}_{bi}$ it applies to the LSS so that the vibration induced to the LSS is minimized while it avoids collisions or undesirable configurations.

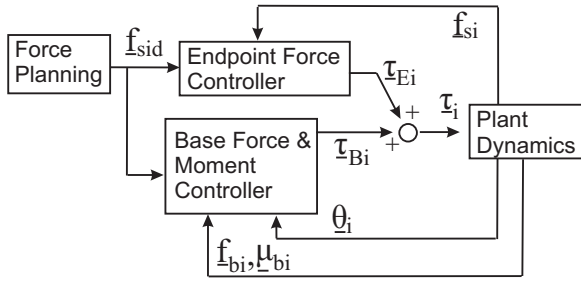


Fig. 4. Overview of the VMR algorithm

For the case considered here, the planning and control algorithms for the forces applied to the module and to the LSS are somewhat different. The endpoint force controller for the forces \underline{f}_{si} calculates joint torques $\underline{\tau}_{Ei}$ for all robots using force measurements from all robots. This form of robot cooperation improves the ability of the robots to control the forces \underline{f}_{si} compared to the case where each robot controls the force it applies to the module independently. The desired forces \underline{f}_{sid} for each robot are planned so that the module is placed accurately, with low residual vibration and the load is distributed evenly among the robots.

Each robot plans and controls independently the reaction forces \underline{f}_{bi} and moments $\underline{\mu}_{bi}$ it applies to the LSS while simultaneously avoids undesirable configurations. The desired reactions \underline{f}_{bid} and $\underline{\mu}_{bid}$ minimize the excitation of vibration in the LSS. This is achieved through a variation of the parallel force/position control scheme in combination with robot motion planning and use of reaction wheels [11].

The total actuation for the robot joints is:

$$\underline{\tau}_i = \underline{\tau}_{Ei} + \underline{\tau}_{Bi} = \underline{J}_{ei}^T \underline{\gamma}_{Ei} + \underline{\tau}_{Bi} \quad (7)$$

where $\underline{\tau}_{Ei}$ and $\underline{\tau}_{Bi}$ are the joint torques for the i-th robot from the endpoint force controller and the base reaction force/moment controller respectively.

4. FORCE PLANNING

This section describes a simple algorithm for the calculation of the desired forces \underline{f}_{sid} that robots are to apply to the module so that it is positioned accurately and with low levels of residual vibration. The initial beam position and orientation are $\underline{r}_{Gs}(0) = \underline{0}$ and $\theta_s(0) = 0$. The desired module position and orientation are $\underline{r}_{Gs}(\Delta t)$, $\theta_s(\Delta t)$, where Δt is the maneuver duration. The j-th component of \underline{f}_{sid} is expressed as a sum of M sinusoids:

$$f_{sjd}(t) = \sum_{k=1}^M \{a_{ijk} \sin(\omega_{pi} t)\} \quad (8)$$

where $i=1,2$ and $j = X,Y$. The frequencies ω_{pi} are chosen to be within the bandwidth of the endpoint force controller. The values of the parameters a_{ijk} are found by imposing the following constraints:

1. The forces \underline{f}_{sid} are always smooth.
2. The forces \underline{f}_{sid} cause the beam to translate by $\underline{r}_{Gs}(\Delta t)$ and rotate by $\theta_s(\Delta t)$.
3. The forces \underline{f}_{sid} induce minimum residual vibration in the beam after the maneuver. This is achieved by imposing the following condition for each one of the beam modes that dominate its vibration response [12]:

$$\|L\{h_i\}\| \equiv \left\| \int_0^{\Delta t} h_i(t) e^{-s_i t} dt \right\| = 0 \quad (9)$$

where h_i is defined in Eq. 6 and s_i is the pole of beam mode i. The condition for robust residual vibration elimination at this mode is:

$$\left\| \frac{dL\{h_i\}}{ds_i} \right\| = \left\| \int_0^{\Delta t} t h_i(t) e^{-s_i t} dt \right\| = 0 \quad (10)$$

The modes that dominate the beam vibration response when the beam is excited at its ends by the forces \underline{f}_{si} are selected as the modes with the highest Hankel singular values [13].

For small angles θ_s , the imposed conditions form a linear system $\underline{A}_p \underline{a} = \underline{b}_p$ where \underline{A}_p , \underline{b}_p are coefficient matrices and \underline{a} contains the unknown parameters a_{ijk} . The solution of this system is obtained by using the pseudo-inverse of \underline{A}_p [10].

This force planning approach is computationally efficient and provides smooth force profiles. Residual vibration elimination can also be achieved by input shaping [14]. The method described in this section is somewhat more general than input shaping because it can deal with nonzero initial vibration conditions. It also can be run on-line to provide updated force commands without inducing time delays.

5. FORCE CONTROL DESIGN

5.1 Endpoint Force Controller

This section describes the design of the endpoint force controller that controls the forces \underline{f}_{-si} robots apply to the module in order to track the commands \underline{f}_{-sid} . The design is based on a linearized nominal model of the robot-beam dynamics, obtained for some robot configuration (where \underline{B}_{Ai} and \underline{D}_{Ai} are constant):

$$\begin{aligned} \dot{\underline{x}}_F &= \underline{A}_F \underline{x}_F + \underline{B}_F \begin{bmatrix} \underline{\gamma}_1 \\ \underline{\gamma}_2 \end{bmatrix} \\ \begin{bmatrix} \underline{f}_{-s1} \\ \underline{f}_{-s2} \end{bmatrix} &= \underline{C}_F \underline{x}_F \end{aligned} \quad (11)$$

where \underline{x}_F is the system state. The vectors $\underline{\gamma}_i$ are defined in Eq. 2 and 3. The plant zeros are the poles of the free-free beam. The plant poles are the poles of the total robots-beam system. Since space structures have poor modal damping, the system poles and zeros are located very close to the imaginary axis. If each robot controls independently its interaction force \underline{f}_{-si} by a P-I controller (force controllers usually contain P and I terms to avoid the differentiation of noisy force signals) the closed loop performance is poor because controller gains must be kept too small to avoid making the closed loop system unstable.

This problem is overcome by the controller design shown in Fig. 5. The endpoint force controller consists of a state feedback controller (centralized controller) combined with the individual PI controllers that each robot uses to control its \underline{f}_{-si} . The centralized control action uses measurements of \underline{f}_{-si} from all robots to calculate joint torques for all robots:

$$\begin{bmatrix} \underline{C} \underline{\gamma}_{E1}^T & \underline{C} \underline{\gamma}_{E2}^T \end{bmatrix} \underline{v} = -\underline{K}_F \underline{x}_F \quad (12)$$

where $\underline{C} \underline{\gamma}_{Ei}$ is the part of $\underline{\gamma}_{Ei}$ (see Eq. 7) that corresponds to the centralized part of the controller. The

system state \underline{x}_F is estimated from measurements of \underline{f}_{-si} . The centralized part of the controller exploits robot cooperation to modify the dynamics of the robots-module system. This allows the application of larger gains in the PI controllers of each robot that improve closed loop performance.

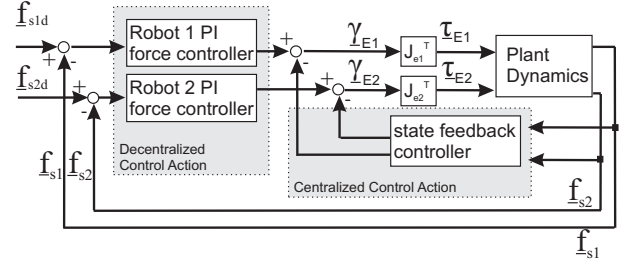


Fig. 5. Endpoint force controller

The robustness of the closed loop performance to the configuration dependent inertial properties of the robots is achieved in two ways. The first is the application of an active damping term:

$$\underline{\tau}_{damp} = -\underline{J}_{ei}^T \underline{D}_{Aid} \underline{J}_{ei} \dot{\underline{\theta}}_i \quad (13)$$

where \underline{D}_{Aid} is the desired damping for robot i , see Eq. 2. The second is to minimize the robot inertia seen by the beam. This is achieved by a multi-link robot design where the majority of its weight is concentrated in its middle link and by exploiting robot redundancy to avoid certain robot configurations (for example singular ones).

5.2 Base Reaction Force/Moment Controller

This section describes the closed loop controller for the reaction forces \underline{f}_{-bi} and torques $\underline{\mu}_{bi}$ applied by each robot to the LSS. It is assumed that the LSS initially has negligible vibration. It is desired to keep the vibration small by eliminating the reactions \underline{f}_{-bi} and $\underline{\mu}_{bi}$ in the directions that induce significant vibration in the LSS. For the case considered here, this is the direction normal to the plane of the LSS, see Fig. 3b.

The design of the base reaction force controller is different than the design of the endpoint force controller (section 5.1). Each robot applies a closed loop scheme to control its own reaction forces and to avoid undesirable joint configurations. The controller is shown in Fig 6, and is a variation of the parallel force/position control scheme [11].

Each robot controls the motion of its redundant joints $\underline{\theta}_i$ and its reaction wheels $\underline{\psi}_i$ by simple joint PD controllers. Since each robot controls already the two

components of \underline{f}_{-si} , it has the freedom to control the N-2 remaining joints. The closed loop force/moment action is achieved by “translating” the error between the desired and the actual base reaction forces and moments into a change in the desired joint acceleration $\ddot{\underline{\theta}}_{id}$ through a PI controller.

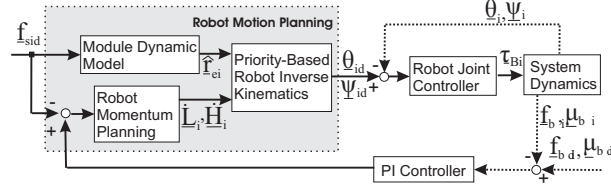


Figure 6: Base reaction force/moment controller

The commands for the robot joint motion $\underline{\theta}_{id}$ and the robot reaction wheel motion $\underline{\psi}_{id}$ are calculated through a priority-based inverse kinematics algorithm [10]. The algorithm priorities are:

1. The robot end-effector velocity matches the estimated motion $\hat{\underline{r}}_{ei}$ of the corresponding beam end that is induced by the planned forces \underline{f}_{sid} .

$$\hat{\underline{r}}_{ei} = \underline{J}_{ei} \dot{\underline{\theta}}_{id} \quad (14)$$

2. The momentum of the robots-module system remains constant. The momentum of each robot is approximated through a Jacobian \underline{J}_{Ri} as:

$$\begin{bmatrix} \underline{L}_i \\ \underline{H}_i \end{bmatrix} = \underline{J}_{Ri} \begin{bmatrix} \dot{\underline{\theta}}_i \\ \dot{\underline{\psi}}_i \end{bmatrix} \quad (15)$$

Then $\underline{\theta}_{id}$, $\underline{\psi}_{id}$ are planned so that the derivative of robot momentum equals the effective forces and moments at the robot CM due to the force applied by the module to the robot $-\underline{f}_{-si} \approx -\underline{f}_{sid}$:

$$\begin{bmatrix} -\underline{f}_{sid} + \underline{f}_{BCL} \\ -\underline{r}_{Gei} \times \underline{f}_{sid} + \underline{\mu}_{BCL} \end{bmatrix} = \underline{J}_{Ri} \begin{bmatrix} \ddot{\underline{\theta}}_{id} \\ \ddot{\underline{\psi}}_{id} \end{bmatrix} \quad (16)$$

where \underline{f}_{BCL} , $\underline{\mu}_{BCL}$ are the outputs of the base reaction force/moment PI controller.

3. The robot avoids undesirable configurations.

Each robot can control the forces \underline{f}_{-si} while eliminating base reaction forces \underline{f}_{-bi} if it is able to vary its linear momentum according to Eq. 16. Assuming slow robot base motions, the robot momentum is expressed as:

$$\underline{L}_i = m_i \cdot (-\ddot{\underline{r}}_{Gbi}) \quad (17)$$

This ability is limited by the size of the locus of reachable locations for the robot CM (CM-workspace) \underline{r}_{Gbi} . The size of the CM-workspace is larger for robots that have many links and concentrate their weight in a single heavy middle link. The elimination of base reaction moments $\underline{\mu}_{bi}$ is improved by using reaction wheels that do not have workspace constraints although they can be limited by actuator torque and speed limits.

6. SIMULATION RESULTS

6.1 System Description

The performance of the VMR controller is evaluated by simulating a planar manipulation of a beam-like flexible module by two robots, see Fig. 2. The properties of each robot are shown in Table 1. Each robot has force/torque sensors in both end-effectors and a reaction wheel at its middle link, see Fig. 7.

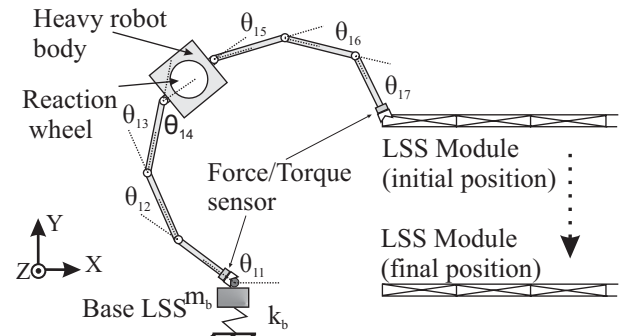


Fig. 7. The planar system used in simulations. Only one of the two robots that manipulate the beam is shown.

Table 1: Robot properties

Number of links:	7
Link length [m]:	[3, 3, 3, 2, 3, 3, 3]
Link mass [kg]:	[18, 18, 18, 242, 18, 18, 18]
Reaction wheel inertia [kg·m ²]	20

The module is modelled as an Euler-Bernoulli beam. The properties of the beam considered in the simulations are shown in Table 2.

Table 2: Beam properties

Length [m]:	200
Young's modulus [GPa]	0.159
Linear density [kg/m]:	3
Lowest vibration modes [Hz]	$f_1=0.197, f_2=0.539, f_3=1.042$

The robot base structure is considered rigid in the X direction and compliant in the Y direction. The base dynamics in the Y direction are modelled by a mass m_B of 2000 kg and a spring rate k_B of 20 N/m, Fig. 7.

The robots manipulate the beam from its initial position $\underline{r}_{Gs}(0)$, $\theta_s(0)$ to its final desired position $\underline{r}_{Gs}(\Delta t)$, $\theta_s(\Delta t)$ within time Δt . The parameters of the simulated manipulation task are shown in Table 3. The design of the robot controller is based on the specifications shown in Table 4.

Table 3: Manipulation parameters

Beam initial position $\underline{r}_{Gs}(0)$ [m]	[0,0] ^T
Beam desired position $\underline{r}_{Gs}(\Delta t)$ [m]	[0,-6] ^T
Beam initial orientation $\theta_s(0)$ [deg]	0
Beam desired orientation $\theta_s(\Delta t)$ [deg]	0
Manipulation duration Δt [sec]	40

Table 4: Controller design specifications

Position error of $\underline{r}_{Gs}(\Delta t)$ [m]	± 0.1
Orientation error of $\theta_s(\Delta t)$ [deg]	± 0.05
Residual vibration at beam ends [m]	± 0.1
Residual vibration at robot base [m]	± 0.1

6.2 VMR Controller Design

The VMR algorithm, Fig. 4, consists of an endpoint force controller for the forces applied by the robots to the module, and a base reaction controller for the robot base reaction forces/moments and joint motions.

Table 5 provides the poles that are used to calculate the gain \underline{K}_F for the centralized part of the endpoint force controller. Table 5 also provides the position of the corresponding poles of the free-free beam.

Table 5: Desired poles of the robots-module dynamics

Free-free Beam Poles	Desired poles for the design of the gain \underline{K}_F
$s_1 = -0.0116 \pm 1.1643i$	$s_1 = -0.6 \pm j$
$s_2 = -0.0321 + 3.2094i$	$s_2 = -0.5 \pm 2.9j$

The input of the centralized force controller is filtered by a low-pass filter to avoid spill-over effects [15]. The cut-off frequency of the filter is $\omega_{bs} = 4.5$ rad/sec:

The decentralized part of the endpoint force controller consists of PI controllers for each component of \underline{f}_{si} .

The beam is considered rigid along the X direction and flexible along the Y direction. Therefore, different PI controllers G_{CFX} , G_{CFY} were used to control the X and Y components of \underline{f}_{si} :

$$G_{CFX} = \frac{0.88s + 0.08}{s^2}$$

$$G_{CFY} = \frac{0.75s + 0.5}{s^2}$$

The active damping added by each robot to the system, Eq 13, corresponds to the damping matrix:

$$\underline{D}_{Aid} = \begin{bmatrix} 50 & \\ & 200 \end{bmatrix}$$

The parallel force/position controller for the base reaction forces and torques consists of joint PD controllers for the robot redundant degrees of freedom and a PI controller for each component of base reactions, Fig 6. The PD joint controller gains for the first joints of the robot are $\underline{K}_{PM} = 1000[38 \ 22.7 \ 12 \ 6 \ 4]$ and $\underline{K}_{DM} = 1000[14 \ 8.4 \ 7 \ 6 \ 4]$. The PD gains for the reaction wheel control are $k_{Pw} = 200$ and $k_{Dw} = 500$. The PI controllers for each component of the base reaction forces and moments are:

$$G_{CFB}(s) = 1 + \frac{10}{s}$$

6.3 Simulation Results

The robot design used in the simulations has a large number of joints and the majority of its weight is concentrated in a single middle link, the robot body. This design has two desirable effects. The first is that the beam feels a very light robot as long as the robot avoids configurations where its last two joints are concurrently smaller than 30 degrees. This makes the robot able to control faster commands. The second is that the CM-workspace of the robot is relatively large, roughly a circle with radius 9m. This makes easier for the robot to eliminate its base reaction forces while controlling the forces it applies to the module, see Section 5.2.

Fig. 8 shows the calculated forces \underline{f}_{sid} that each robot is commanded to apply to the module. Each force component is planned as a sum of M=20 sinusoids. The obtained force command \underline{f}_{sid} is smooth and as expected results in accelerating and then decelerating the beam. Fig. 8 also shows the simulation results for the forces \underline{f}_{si} using the VMR algorithm. The delay between the commands \underline{f}_{sid} and the response \underline{f}_{si} is generally less than 1 sec.

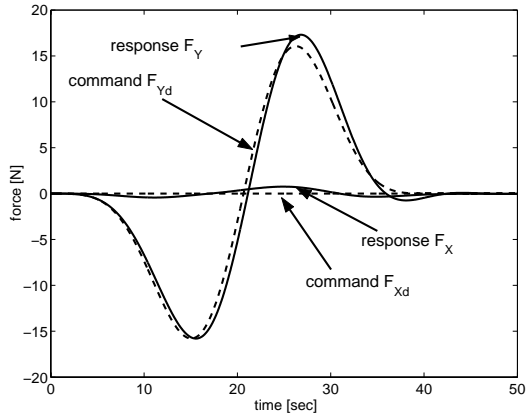


Fig. 8. Force commands \underline{f}_{sid} and actual force response \underline{f}_{si} using the VMR method.

The endpoint controller tracks the commanded forces \underline{f}_{sid} well enough to position the beam within the required position accuracy. Fig. 9 shows the response of the beam motion using the VMR method and the response of the beam when the beam is driven by ideal forces equal to \underline{f}_{sid} . Fig. 9a shows the response of the beam CM motion. Fig. 9b shows the response of vibration deflection at the beam ends. The difference between the ideal case and the results using the VMR algorithm is small.

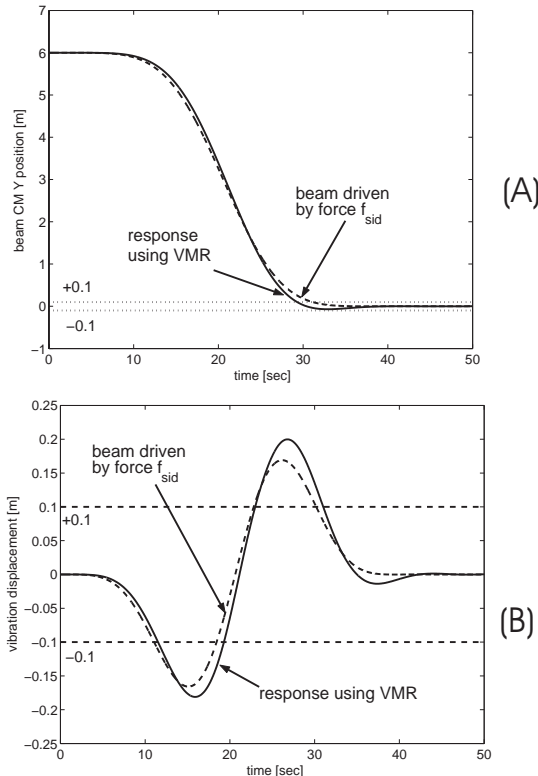


Fig. 9. a) Position response of the beam CM and b) vibration deflection at the left beam end.

In this case, where the base is assumed to be rigid along the X direction, each robot needs to control only the Y component of its base reaction force. The desired command is $f_{biYd} = 0$. Each robot uses its reaction wheel to reduce the magnitude of the torque it applies to the LSS. In the general three dimensional case robots could control all the components of \underline{f}_{bi} and $\underline{\mu}_{bi}$.

Fig. 10 and 11 show the effectiveness of the VMR algorithm in eliminating base reaction forces and moments. They show simulation results using the VMR algorithm when the whole algorithm is used and when the base reaction controller is not used. Fig. 10 shows simulation results for the Y component of robot 1 base reaction force f_{b1Y} . If no base force control is applied, the magnitude of the base reaction force is somehow larger than the magnitude of the command \underline{f}_{sid} for this robot. Fig. 11 shows simulation results for the base reaction torque of robot 1. Fig. 10 and 11 show that the VMR algorithm eliminates the Y component of the reaction force and reduces the magnitude of the torque applied to the base.

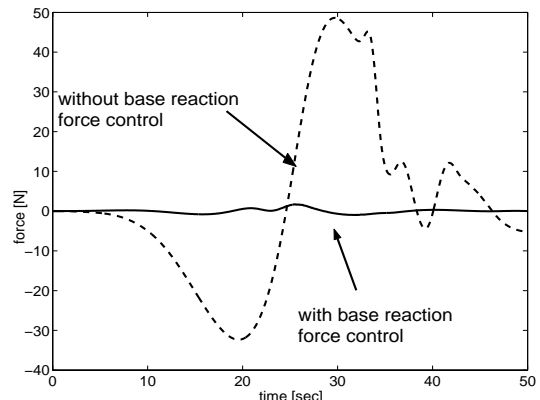


Fig. 10. Reaction force applied to robot 1 by the LSS

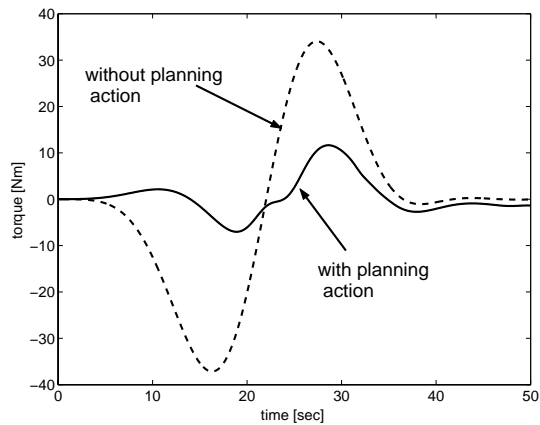


Fig. 11. Reaction torque applied to robot 1 by the LSS

Fig. 12 shows simulation results for the position response of robot 1 base with and without base force control. When the base reaction forces are not controlled they cause large displacements in the compliant LSS. These displacements may force the robot to get into undesirable configurations that deteriorate significantly the performance of the endpoint force controller, Fig. 13. In this case robots fail to position the beam accurately. The base reaction force controller of the MVR algorithm results in small base reaction forces/moments that induce small vibration in the robot base, Fig. 12. This allows the successful control of the forces f_{si} that robots apply to the module, see Fig. 8.

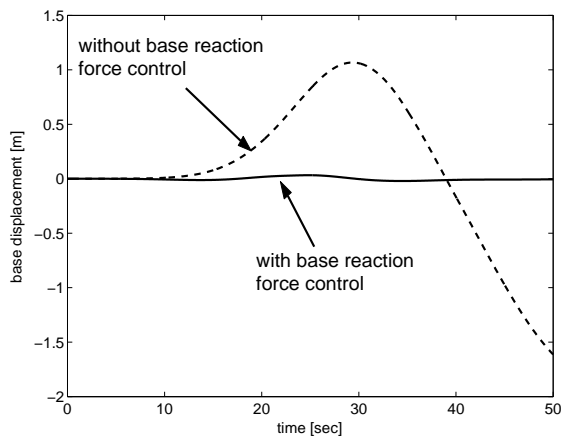


Fig. 12. Base displacement response of robot 1 with and without base reaction force control

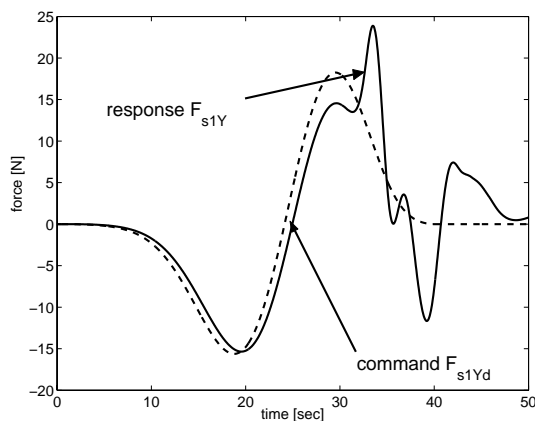


Fig. 13. Command force f_{s1Yd} and response f_{s1Y} when the base reaction forces are not controlled.

7. SUMMARY

This paper describes an algorithm for the manipulation of large flexible structural modules by a team of redundant robots that are mounted on flexible base structures. The algorithm plans and controls cooperatively the forces applied by the robots to the

module in order to maneuver the module accurately and with low residual vibration. The algorithm also minimizes vibration excitation in the compliant robot base structures by using a closed loop controller and exploiting robot redundancy.

8. ACKNOWLEDGEMENTS

This work is sponsored at MIT by the Japanese Aerospace Exploration Agency (JAXA). The authors would like to thank Dr. Matt Lichter and Peggy Boning for their helpful comments.

9. REFERENCES

1. M. Oda et al, Study of the Solar Power Satellite in NASDA, *Proc. of i-SAIRAS 2003*, Nara, Japan, May 2003
2. W. Whittaker et al, Robotics for Assembly, Inspection, and Maintenance of Space Macrofacilities, *AIAA Space 2000 Conference*, Reston VA, September 2000
3. Senda K. et al, Hardware Experiments of Space Truss Assembly by Autonomous Space Robot, *AIAA Guidance, Navigation and Control Conference*, Denver CO, August 2000
4. Doggett W., Robotic Assembly of Truss Structures for Space Systems and Future Research Plans, *IEEE Aerospace Conference 2002*, Vol. 7, March 2002, pp. 3584 – 3598
5. Yakawa T. et al, Stability of Control System in Handling of a Flexible Object by Rigid Arm Robots, *1996 IEEE International Conference on Robotics and Automation*, Minneapolis MN, pp. 2332-2339, April 1996.
6. Torres, M. and Dubowsky, S., Path Planning for Elastically Constrained Space Manipulator Systems, *1993 IEEE International Conference on Robotics and Automation*, Atlanta GA, Vol. 1, pp. 812-817, May 1993.
7. Yoshida et al, Vibration Suppression and Zero Reaction Maneuvers of Flexible Space Structure Mounted Manipulators, *Smart Mater. Struct.*, 8, 1999, pp. 847-856
8. Khatib O., Inertial Properties in Robotic Manipulation: An Object-Level Framework, *The International Journal of Robotics Research*, Vol. 13, No. 1, February 1995, pp. 19-36
9. Meirovich L., *Methods of Analytical Dynamics*, Dover Publications, 1998
10. Nakamura Y., *Advanced Robotics; Redundancy and Optimization*, Addison-Wesley Publishing, 1991
11. Chiaverini S., Siciliano B., The Parallel Approach to Force/Position Control of Robotic Manipulators, *IEEE Trans. Automatic Control* 1993, 39, pp. 647-652
12. Bhat S. and Miu D., Precise Point-to-Point Positioning Control of Flexible Structures, *ASME Journal of Dynamic Systems, Measurement and Control*, December 1990, Vol. 112, pp. 667-674
13. Gawronski W., *Dynamics and Control of Structures; a Modal Approach*, Springer, 1998
14. Singer N.C., Seering W.P., Preshaping Command Inputs to Reduce System Vibration, *ASME Journal of Dynamic Systems, Measurement and Control*, March 1990, Vol. 112, pp. 76-82
15. Balas M., Feedback Control of Flexible Systems, *IEEE Transactions on Automatic Control*, Vol. 23, No. 4, August 1978